Earthquake Engineering, Tenth World Conference © 1992 Balkema, Rotterdam. ISBN 90 5410 060 5

Bond decay of beam bars in joint region under load reversals

Sh. Morita & Sh. Fujii
Kyoto University, Japan

H. Murakami
Konoike Co., Osaka, Japan

T. Yamada
Kajima Co., Tokyo, Japan

ABSTRACT: In order to add the fundamental knowledge on bond between high strength concrete and high strength rebars, full-scale tests were performed by using a new type test method. This test method aimed at reproducing the real pull-push condition of a beam bar in an interior beam-column joint under earthquake type loadings. Test variables in this study were (1) concrete strength varied up to 120 MPa, (2) yield stress of bars up to 700 MPa, (3) bar diameter up to 35mm, (4) column depth and unit width per beam bar, (5) column axial stress. From the test results, the maximum local bond stress within the confined region could be formulated as a function of these test variables. Bond index defined in this study by the use of this maximum bond stress gave a good measure to grade the degree of bond deterioration under load reversals.

1 INTRODUCTION

In order to develop a seismic design guideline for advanced reinforced concrete buildings using high-strength materials, it is required to add test data on bond capacity between high strength concrete and beam bars passing through interior beam-column joints. The present design provisions of building codes for development of beam bars stress within the joint region often requires to keep the minimum column depth versus bar diameter ratio. Though this ratio strictly limits the size of columns, the basis for this provision is not so obvious as to extrapolate to high-strength materials.

Experimental studies performed on beam-column subassemblages are generally not appropriate to focusing on the bond behavior in joints, because it is difficult to exclude the effects due to other influencing factors from the total behavior. So, a new simple test method was developed to reproduce the real stress condition of beam bars in the joint region. By using this test method, fourteen specimens were tested to add the quantitative basis of the design provision for bond in joints.

2 EXPERIMENTAL PROGRAM

2.1 *Test specimens*

To simplify the fabrication of test specimens and also to reproduce the actual stress condition in the joint region, the specimens in this study were configured to the shaded portion of a beam-column subassemblage shown in Figure 1. It is notable that a concrete stub protruding from each column face was provided to simulate the stress state in the beam hinging region. These concrete stubs played the important roll in distrubuting total applied load P to steel force Ps and concrete resultant force Pc.

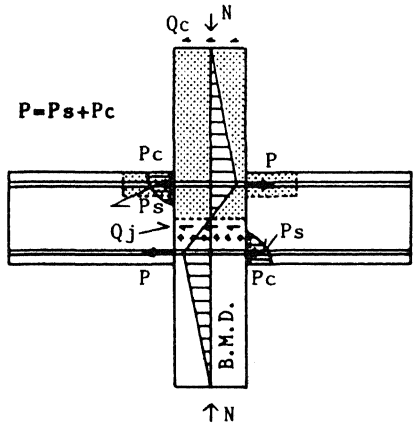

Fig. 1 Simulated portion of beam-column subassemblage by test specimens

Figure 2 shows the details of two types of specimens. The smaller one and the larger one *were designated as, S type and L type,* respectively.

Beam bars having proof yield stress of 700 MPa used in this study was newly developed for the practical application to the advanced reinforced concrete system. Screw type bars

were used for test beam bars. Column portions having unit width per beam bar were reinforced axially by eight 16 mm dia. deformed bars having 700 MPa proof yield stress, and but-welded closed hoops of 8 mm dia. indented bars arranged as shown in Figure 2 at 60 mm on centers were used as lateral reinforcement for every specimen. Protruding concrete stubs were reinforced by a 30 mm pitch spiral of 9 mm dia. bar to avoid premature splitting or compressive failure.

Table 1 summarizes the description of test specimens. Test variables were: column depth (D=400, 600 mm), diameter of beam bars (db=19, 25, 35 mm), proof yield stress of beam bars (fy=35, 70 MPa), compressive strength of concrete (fc'=40, 80, 120 MPa) and column axial stress strength ratio

Table 1 Descriptions of test specimens

Number	Designation[1)]	Column section B × D mm × mm	Beam bar db mm	Steel yield stress fy MPa	Concrete strengh fc' MPa	Column axial load N kN	(N/BDfc')
No. 1	S-19-700- 40-1/6		19	770	41.8	245	(1/6)
No. 2	S-19-700- 80-1/6		19	770	81.8	539	(1/6)
No. 3	S-19-700-120-1/18		19	770	123.4	245	(1/18)
No. 4	S-25-700- 40-1/6		25	711	34.6	245	(1/6)
No. 5	S-25-700- 80-1/6	100 × 400	25	711	93.2	539	(1/6)
No. 6	S-25-350- 40-1/6		25	373	36.1	245	(1/6)
No. 7	S-19-700- 40-1/3		19	770	43.4	537	(1/3)
No. 8	S-19-700- 80-1/3		19	770	81.8	1080	(1/3)
No.13	S-25-700-120-1/6		25	710	127.2	785	(1/6)
No. 9	L-25-350- 40-1/6		25	373	35.0	588	(1/6)
No.10	L-25-700- 80-1/6		25	704	98.9	1180	(1/6)
No.11	L-25-700- 40-1/6	150 × 600	25	710	35.0	588	(1/6)
No.12	L-35-350- 80-1/6		35	359	96.6	1180	(1/6)
No.14	L-35-700- 80-0		35	753	85.6	49	(0)

Note 1) Designation S- 19-700- 40-1/6

- Column axial stress lebel [0, 1/18·fc', 1/6·fc', 1/3·fc']
- Concrete strengh [40, 80, 120(MPa)]
- Steel yield stress [350, 700(MPa)]
- Beam bar diameter [19, 25, 35(mm)]
- Size of specimens [S:B×D=100×400, L:B×D=150×600(mm)]

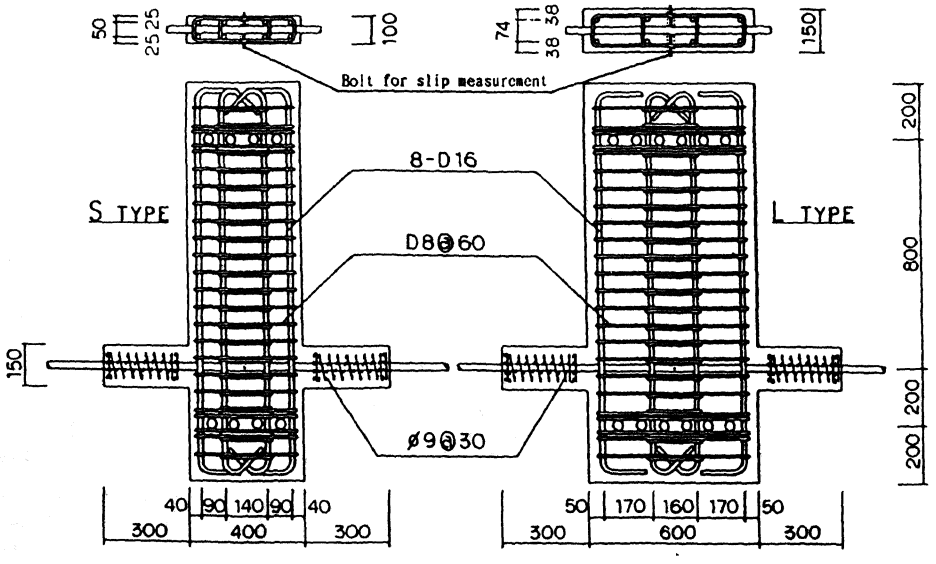

Fig. 2 Details of test specimens

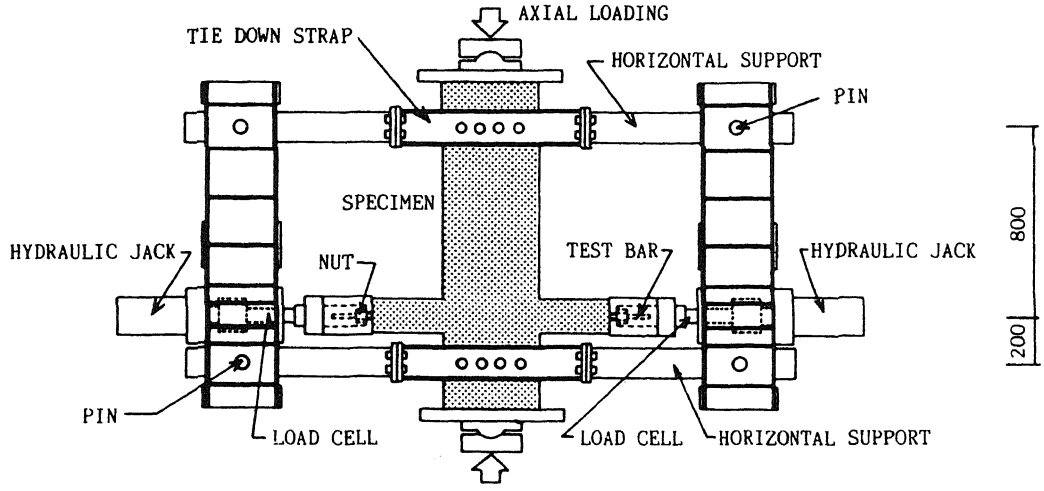

Fig. 3 Loading apparatus

(N/BDfc'=1/3, 1/6, 1/18, 0).

2.2 Loading Method

The loading apparatus shown in Figure 3 was used in this study. After applying the column axial load N, pull-out force P was applied at the end of the beam bar and push-in force of equal magnitude was applied simultaneously at the opposite end surface of the concrete stub. From this manner of loading, the stress distribution similar to what existed along beam bars passing through interior beam-column joints was given. Reversed cyclic pull-push loading at beam bar ends was given at a constant increment of the load amplitude up to yielding of the beam bar, and then continued almost at a constant increment of the peak strain of the beam bar in pull loading up to just before tensile fracture of the bar, if bond failure didn't occur.

2.3 Measuring instrumentation

Slip of the test bar at the center of the joint S_2 and at the column faces S_1 and S_3 was successfully measured with reference to the central portion of joint core concrete by using special instrumentation. Steel strain was measured by wire-resistance strain gages installed to the test bar at the intervals of 100 mm (at 50 mm intervals in the neighborhood of column faces).

3 TEST RESULT

In the case of bond failure, loading was stopped at the limit slip of 10 mm. In some cases where excessive bond deterioration took place, the concrete stub in compression was crushed, because the pull-out force could not be transferred within column depth and gave some additional compressive force to that stub. No.4 specimen failed in shear at the joint region.

Figure 4 shows the typical crack pattern of No.5 specimen which failed in bond. Longitudinal cracking along the beam bar observed in Figure 4 did not appear at all in any specimen, which did not fail in bond including highly loaded one up to almost tensile strength beyond yielding.

Figure 5 shows a typical example of the applied load versus slip relationship observed in the specimen which failed in bond after several cycles of reversed loading in post-yield range. Inward local slip observed at the column face was quite small in comparison with outward local slip at this location before the commencement of bond deterioration. At the midway of the column depth, slip of equal magnitude in both directions was always observed.

With the progress of bond deterioration due to load reversals, inward slip gradually increased and complete bond failure was observed soon after. These procedures are clearly explained by Figure 5.

In Figure 6, $(S_1 + S_3)$ was plotted against $(P_1 - P_3)$ for each loading step for some specimens, where P_1 or P_3 denotes the applied load at each end simultaneously (positive in

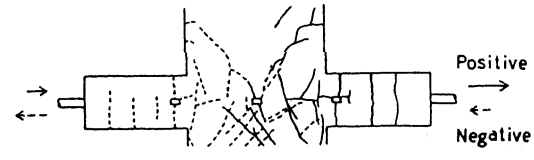

Fig. 4 Crack patterns observed at No.5 specimen which failed in bond

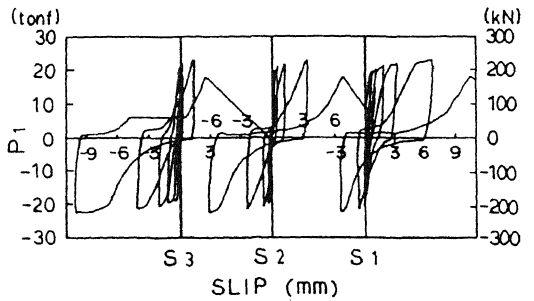

Fig. 5 Load - slip curves of No.6 specimen that failed in bond

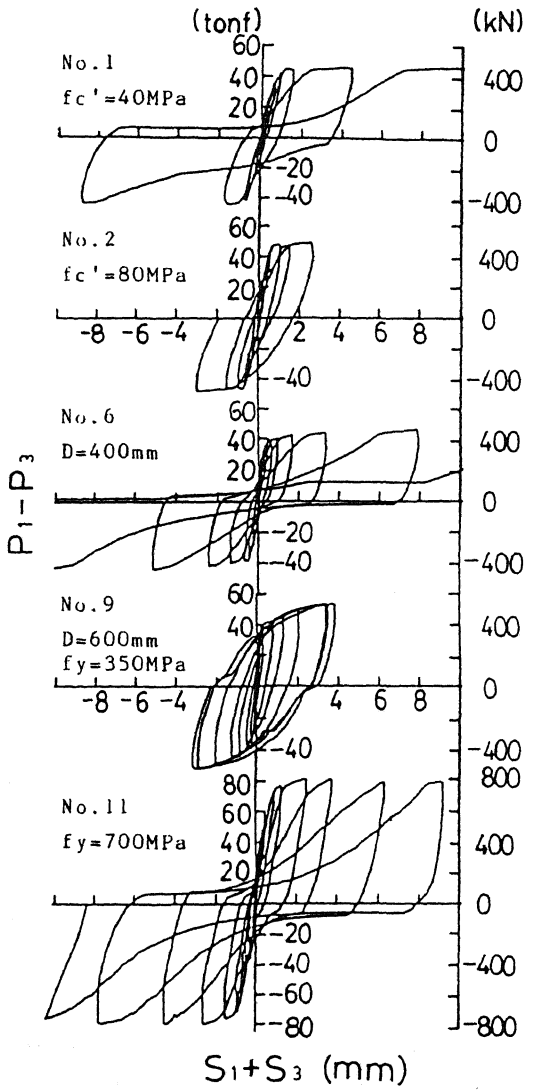

Fig. 6 (P_1- P_3) versus (S_1+ S_3) curves

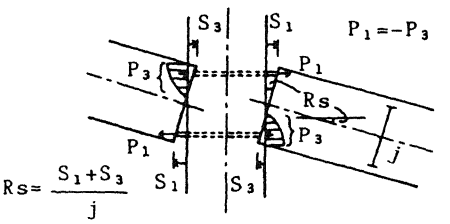

Fig. 7 Additional deformation due to slip at column face

tension) and S_1 or S_3 denotes the corresponding local slip at the column face. The value of (P_1 -P_3), equal to $2P_1$ in these cases, is almost proportional to applied moment at a beam end as shown in Figure 7. Then, (S_1 +S_3) is also proportional to the additional rotation due to pull-out and push-in slippages of the beam bar at the column face as explained in Figure 7.

Therefore, (P_1 -P_3) versus (S_1 +S_3) curves may be assumed to represent moment versus additional rotation curves at column faces of interior beam-column joints.

As shown in Figure 6, the moment versus additional rotation curves derived from specimens (No.1, No.6 and No.11) which failed in bond indicate the rapid increase of additional rotation and the pinched hysteresis under load reversals. On the contrary, the curves obtained from specimens (No.2 and No.9) which did not fail in bond exhibited stable and fat hysteretic curves. Figure 6 reveals that the total bond ability within the joint region is improved with the increase of concrete strength and column depth and with the decrease of yielding stress of rebars. Table 2 summarizes the failure mode of each specimen.

4 LOCAL BOND - SLIP CURVES

From the measured steel strains at the intervals of 100 mm at the central part and 50 mm at the column faces, local bond stress versus slip curves (τ-s curves) could be derived. Observed strains after load reversals in inelastic range were transformed to stresses by using the Ramberg-Osgood function. This estimation could be calibrated from the readings of load cells located at the ends of the beam bar. Local bond stresses were given as the average bond stresses over adjacent strain-measured locations. Local slip at a location could be obtained by adding the calculated elongation of bars, integrated strain over distance from the location to the column center, to the observed slip at the column center without considering concrete deformation.

Figure 8 shows the τ-s curves obtained at several locations within the joint region. The curves obtained within core concrete were

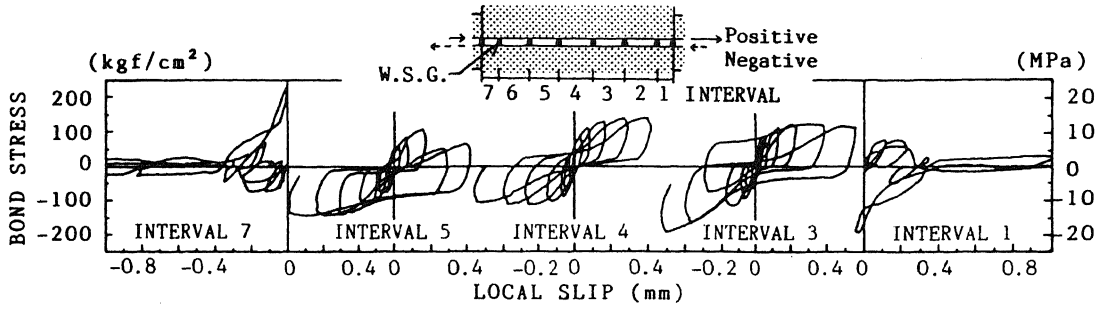

Fig. 8 Local bond stress - slip curves of No.9 specimen

quite differ from that obtained at the neighborhoods of column faces i.e. at the cover concrete. The almost equal magnitude of local bond stress in both directions could be seen within the core concrete, while in the cover concrete the low bond stress was developed in the outward direction and the extremely high bond stress could be obtained in the inward direction, but only at the lst cycle after yielding in tension at the previous cycle. This characteristic performance in bond can be explained as the result of the crack opening and closing mechanism in the joint.

Envelopes of τ-s curves observed in the core region are shown in Figure 9 grouping them into three to show the influence of each main test variable. It is recognized that the increase in concrete strength or column axial force gave higher local bond strength and higher rigidity of τ-s curves. It is also shown in Figure 9(c) that the local bond strength was increased with the increase of specimen width versus beam bar diameter ratio and that column depth is not a decisive factor for the local bond strength. Based on the tendency of test results shown in Figure 9, the local bond strength τu could be formulated from the regression analysis as:

$$\tau u = 2.2\,(0.86 + 0.84\frac{N}{BDfc'})\cdot\frac{B}{db}\cdot(\frac{fc'}{35})^{0.66} \quad (1)$$

(in MPa)

In applying Eq.(1), the estimation of the B/db effect should be limited within the variation tested in this study.

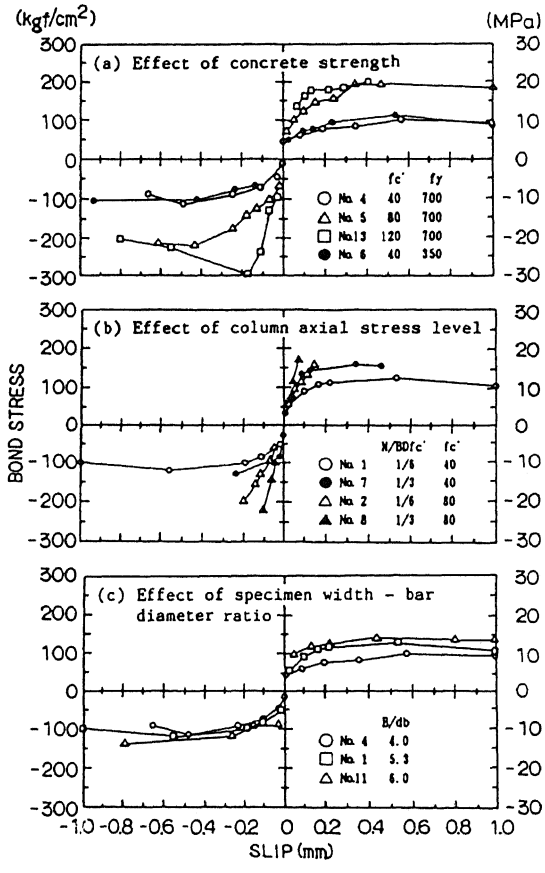

Fig. 9 Envelopes of local bond stress - slip curves in core region

5 BOND INDEX FOR DESIGN OF JOINTS

Design Guidelines of AIJ (1990) recommends to provide the column depth of weak-beam and strong-column frames greater than Dcal defined as:

$$Dcal = \frac{1}{10}\cdot\frac{fy\cdot db}{\sqrt{fc'}} \quad (2)$$

The average bond stress τf required for a beam bar to develop tensile yielding at the front face and compressive yielding at the far face of an interior column is:

$$\tau f = \frac{fy\cdot db}{2\,D} \quad (3)$$

In this study, τu/ τf was defined as the bond index which gave a scale to measure the

Table 2 Failure mode and bond indices.

Number	Failure mode[1)]	D/Dcal	τu/τf
No. 1	B-SL	0.55	0.70
No. 2	C	0.77	1.10
No. 3	C	0.95	1.31
No. 4	A-SH	0.41	0.39
No. 5	B-CC	0.68	0.73
No. 6	B-CC	0.81	0.77
No. 7	B-SL	0.56	0.82
No. 8	C	0.77	1.26
No.13	B-CC	0.80	0.91
No. 9	C	1.19	1.71
No.10	C	1.06	1.72
No.11	B-CC	0.63	0.90
No.12	C	1.47	1.73
No.14	D	0.66	0.68

Note 1) Failure mode

B- SL

- SL : Excessive slip up to ±10mm.
- CC : Compressive failure of concrete stub.
- SH : Shear failure of joint region.
- A : Bond failure before yield.
- B : Bond failure within three cycles of reversed loading in post-yield range.
- C : No bond failure within above-mentioned loading cycles.
- D : Discontinue before bond failure due to shortage of Loading capacity.

ability of bond in interior column joints.

In Table 2, D/Dcal and τu/ τf for each specimen were summarized along with the remarks on failure modes. These D/Dcal and τu/ τf values were plotted in Figure 10 and the failure modes were indicated by classifying into four groups. In addition to these data summarized in Table 2, nine test results, which were obtained from pull-push loading tests quite similar to the test shown in Figure 3 but without protruding concrete stubs, were also plotted in Figure 10.

Figure 10 indicates that the bond index τu/ τf provides a good measure in comparison with D/Dcal. It is shown that if τu/ τf is kept to be larger than unify, bond failure within three cycles of reversed loading in post-yield range may be avoided.

6 CONCLUSIONS

A new test method for the investigation of bond behavior of beam bars in interior beam-column joints under earthquake-type loading was developed. From the test results in this study, following conclusions could be obtained:

1. The adopted new type test method could reproduce the bond behavior of beam bars in beam-column joints.
2. Bond deterioration under load reversals was accelerated by yield elongation of the bar.
3. Local bond stress versus slip relationships in confined core region was quite different from that in unconfined cover region.
4. Bond index τu/ τf defined and formulated in this study by Eq.(1) and Eq.(3) gave a good measure to judge the bond ability of beam bars in joints.

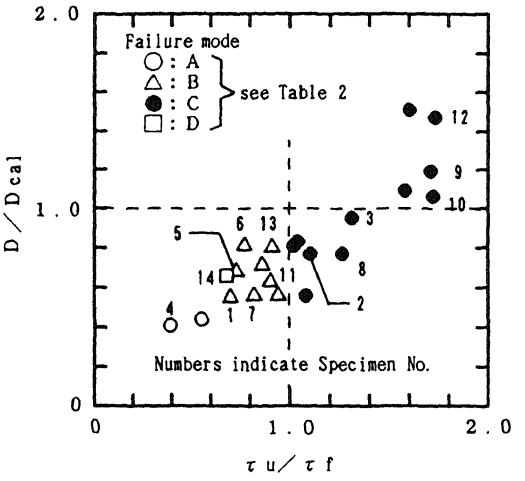

Fig. 10 Grading of failure mode by the bond index

REFERENCES

Aoyama, H. et al. 1990. Outline of the Japanese national project on advanced reinforced concrete buildings with high-strength and high-quality materials, The 2nd International Symposium on Utilization of High Strength Concrete

Architectural Institute of Japan 1990. Design guidelines for earthquake resistant reinforced concrete buildings based on ultimate strength concept

ACKNOWLEDGMENTS

The authors express their gratitude to Mr. Tetsuya Masui, graduate student of Kyoto Univ. for his cooperation. The study was excuted as a part of activities of Japanese national project on advanced reinforced concrete building system introduced by Aoyama (1990).